Electrochemical Tryptophan-Selective Bioconjugation

Ryo Kuroda,[‡1] Eisho Toyama,[‡1] Tomoya Sugai,[2] Maho Imai,[3] Kohei Watanabe,[1,4] Natsuki Konoue,[1] Katsuya Maruyama,[1] Mio Kondo,[3] Shigeyuki Masaoka,[5] Tsuyoshi Saitoh,[2] Kounosuke Oisaki,[1,6,7]* Motomu Kanai[1]*

[1] Graduate School of Pharmaceutical Sciences, The University of Tokyo, 7-3-1 Hongo, Bunkyo-ku, Tokyo 113-0033, Japan
[2] International Institute for Integrative Sleep Medicine (WPI-IIIS), University of Tsukuba, 1-1-1 Tennodai, Tsukuba, Ibaraki 305-8575, Japan
[3] Department of Chemistry, School of Science, Institute of Science Tokyo, NE-6, 2-12-1 Ookayama, Meguro-ku, Tokyo 152-8550, Japan
[4] Faculty of Education, Chiba University, 1-33, Yayoi-cho, Inage-ku, Chiba 263-8522, Japan
[5] Graduate School of Engineering, Osaka University, 2-1 Yamadaoka, Suita, Osaka, 565-0871 Japan
[6] Interdisciplinary Research Center for Catalytic Chemistry (IRC3), National Institute of Advanced Industrial Science and Technology (AIST), Tsukuba Central 5-2, 1-1-1 Higashi, Tsukuba, Ibaraki 305-8565, Japan
[7] Open Innovation Laboratory for Food and Medicinal Resource Engineering (FoodMed-OIL), National Institute of Advanced Industrial Science and Technology (AIST), Tsukuba, Ibaraki, 305-0821, Japan

KEYWORDS: Tryptophan, Bioconjugation, Electrochemistry, Protein, Organoradical.

ABSTRACT: Bioconjugation reactions are a fundamental synthetic strategy for generating artificial peptides and proteins. Although bioconjugates at hydrophobic amino acid residues can offer superior product homogeneity compared to those at hydrophilic residues, methods to target moderately reactive hydrophobic amino acids under mild and metal-free conditions are limited. In this study, we present the first electrochemically promoted, tryptophan (Trp)-selective bioconjugation that is applicable at the protein scale in a neutral buffer. The unique electrochemical cooperation of two radicals, keto-ABNO and 4-oxo-TEMPO, along with NaBr, was key to accelerating the reaction while simultaneously suppressing both anodic overoxidation of the products and cross-reactivity. Systematic cyclic voltammetry (CV) and UV-visible absorption spectroelectrochemistry (SEC) analyses revealed that these two radicals, which have similar redox potentials but differing steric demands, serve distinct electrochemical roles (as reactant and electrochemical mediator, respectively). Additionally, NaBr was suggested not to function as a redox mediator, but instead likely prevents the decomposition of oxoammonium active species. This electrochemical protocol marks a significant advance toward novel processing techniques for chemically modified biologics.

Introduction

Bioconjugation reactions are fundamental synthetic methodologies essential for producing synthetic peptides and proteins. Recent attention has focused on selective bioconjugation methods[1-7] targeting less surface-exposed, hydrophobic proteinogenic amino acids, such as tyrosine,[8-10] tryptophan,[11] and methionine.[12] These methods meet the growing demand for efficient production and expansion of chemical space of homogeneous protein conjugates without genetic manipulations, thus enhancing their property, efficacy and potential applications. Practical bioconjugation reactions require (1) selectivity for a specific functional group within a target proteinogenic amino acid, (2) selective activation of the bioconjugation reagents in the presence of numerous reactive functional groups in biomacromolecule substrates, (3) feasibility under physiological conditions (mild pH and temperature, aqueous media, and low concentration), and (4) avoidance of excess and toxic metallic reagents that could cause undesired cross-reactivities and complicated purification. Meeting these requirements is particularly challenging for less reactive hydrophobic amino acid residues compared to nucleophilic residues like lysine and cysteine.[6]

Integrating electrochemical organic synthesis[13-17] with bioconjugation chemistry is a promising strategy to achieve these goals. Electrochemical single-electron transfer processes are biocompatible energy inputs that enable operability in aqueous media, reduce byproducts, and exhibit high reactivity and functional group tolerance.[18,19] Historically, electrochemical protein modifications at preparative scales have been limited to direct electrolysis for cysteine-cystine interconversions, site-selective cleavage, and oxidative functionalization.[20-23] Since 2018, however, several electrochemical protein bioconjugations targeting tyrosine (Tyr) residues have been reported.[24-28] More recently, electrochemical bioconjugation has extended to tryptophan (Trp) residues at the peptides scale[29] and to affinity labeling of biomacromolecules.[30] In this study, we report first electrochemical Trp-selective bioconjugation operable at the protein scale. The cooperative use of two *N*-oxyl radicals and a bromide source was essential for efficient, high-yielding bioconjugation.

Results & Discussion

In our previous work, we reported a transition metal-free, Trp-selective bioconjugation using a sterically less-

demanding organoradical, 9-azabicyclo[3.3.1]nonan-3-one-*N*-oxyl (keto-ABNO), with substoichiometric $NaNO_2$ in mildly acidic aqueous media (0.1-1% AcOH aq., pH ~ 3).[31,32] The active species in this bioconjugation is the oxoammonium cation **A** (see Figure 10), which is generated *in situ* via single-electron oxidation promoted by nitrogen oxide (NO_x) produced from $NaNO_2$ and AcOH under air. While this approach is straightforward and compatible with a range of substrate, it has some potential limitations: (1) the acidic media, which can impede applications to pH-sensitive proteins, and (2) side reaction induced by NO_x, such as *S*- and *N*-nitrosation. Given the well-established role of *N*-oxyl radicals as electrochemical mediators,[33] we hypothesized that anodic electrochemical oxidation could activate keto-ABNO for Trp-selective bioconjugation in buffered media at neutral pH, eliminating the need for external oxidants (e.g., NO_x), which could lead to undesirable side reactions.

To verify this hypothesis, we conducted optimization studies for the electrochemical bioconjugation of Fmoc-protected pentapeptide **1a** (Fmoc-GSNWG-OH) as a model substrate using an ElectraSyn 2.0 setup (Figure 1a). Without applying and electric current, a mixture of **1a** (3 mM) and keto-ABNO (3 mM) in an electrolyte solution (50 mM tetrabutylammonium perchlorate (TBAP) in CH_3CN-H_2O, 1:1) stirred for 1 hour yielded only 33% of product **2a**, with unreacted starting material (entry 1).[34] However, applying constant voltage electrolysis (working electrode/WE: graphite, counter electrode/CE: platinum, reference electrode/RE: Ag/Ag^+) at 1.2 V for 1.0 F/mol (approximately 1 hour) significantly increased the yield of **2a** to 75%, with 18% of **1a** recovered (entry 2). Further increasing the electric charge led to complete consumption of **1a**, but also an increase in overoxidation byproducts **3a**/**3a'** (entries 3 and 4). At this potential, **2a** is likely susceptible to electrochemical oxidation as well, as indicated by the anodic peak of Trp–keto-ABNO adduct in PBS at 0.98 V *vs* Ag/AgCl, Figure S5). Therefore, lowering the potential to 1.0 V effectively suppressed the overoxidation, though the yield of **2a** dropped to 55% (entry 5). Applying 2.0 F/mol at 1.0 V improved the yield to 78% (entry 6), although further increased in applied charge (>2 F/mol) were limited by rising resistance.

Next, we screened additives to enhance electron-transfer processes. Interestingly, adding sterically demanding 2,2,6,6-tetramethylpiperidine-*N*-oxyl (TEMPO) derivatives significantly increased the yield of **2a** (entries 7–11 *vs.* entries 5 and 6). Since TEMPOs are inert in Trp bioconjugation under NO_x conditions,[31] adducts of TEMPO derivatives with **1a** were undetected in these trials. Among the conditions tested, 0.6 mM of 4-oxo-TEMPO provided the best result, with complete consumption of **1a** and minimal formation of overoxidized byproducts **3a**/**3a'** (97% yield of **2a**, entry 11). The efficiency of the additives correlated with their redox potentials,[35] with higher oxidation potential TEMPO derivatives yielding more **2a**. The current efficiency (the slope of the yield of **2a** *vs.* charge graph, Figure S3) was approximately 1.5 times greater in the presence of 4-oxo-TEMPO than without it.

Further optimizations were conducted in organic solvent-free, aqueous buffered conditions using the water-soluble, N-terminus-unprotected pentapeptide **1b** (H-GSNWG-OH). However, switching to buffered media hindered Trp-selective modification. The ElectraSyn 2.0 setup often encountered unstable electric charge application due to high resistance in the diluted reaction media (0.26 mM of **1b**). Consequently, we switched to an ECStat-301 potentiostat (EC FRONTIER, Co., Ltd) connected to the ElectraSyn electrodes and vial kit for secured reproducibility (Figure S1). Despite this setup, the reaction in PBS buffer only achieved low conversion (3% yield of **2b**, Figure 1b, entry 1). To achieve reagent-selective electrolysis, different electrode combinations were tested. Using glassy carbon (GC) electrodes for both WE and CE improved productivity (37% yield of **2b**, entry 2). Phosphate anions in the buffer may have been detrimental, as switching from PBS to Tris-HCl improved enhanced the reactivity (Table S2). Screening inorganic additives to mitigate the negative effect of phosphate revealed that addition of NaBr (0.78 mM) and lower concentration of 4-oxo-TEMPO (0.26 mM) improved reaction efficiency, yielding 94% of **2b** at 2.0 F/mol charge (entry 4-6). Notably, under the NO_x activation conditions,[31] the transformation of **1b** yielded **2b** in a reduced yield (70%) due to the formation of nitrosated **2b** as a byproduct (17%, entry 7).

Having established the optimal conditions, we next assessed the compatibility of redox-active amino acids. The optimal conditions were applied to model peptide **1b** in the presence of 1 equivalent of various amino acids (Figure 2). The reaction proceeded smoothly with Lys and Met (entries 2 and 3). In the presence of histidine (His), however, the standard voltage resulted in low recovery of His. Lowering the voltage to 0.6 V improved both the product yield and His recovery (entry 1). When Tyr was present, the reaction was slower under standard conditions, but satisfactory yield and Tyr recovery were achieved by increasing the voltage and electric charge (entry 4). Notably, redox-insensitive cystine (Cys dimer) was well-tolerated under these conditions (entry 5).

With amino acid compatibility confirmed, we applied the conditions to commercially available biorelevant peptides containing Trp (Figure 3). To achieve higher conversion, we used a higher concentration of keto-ABNO (1.04 mM, 4 equivalents to the peptides). The reaction proceeded efficiently with leuprorelin, yielding 82% of the adduct. Delta sleep-inducing peptide displayed a slower reaction with concurrent oxidative side reactions; however, by applying increased charge at a lower voltage, we achieved a moderate yield of the keto-ABNO adduct (60%). Somatostatin, which contains a macrocyclic disulfide, afforded the desired adduct in high yield (89%). Octreotide, featuring both a cyclic disulfide and a C-terminal threoninol moiety, showed good reactivity (81%), even with modification at an unnatural D-Trp residue. Daptomycin, an antimicrobial lipopeptide produced by a non-ribosomal pathway, also showed good yield (76%) with an increased amount of keto-ABNO.

A significant advantage of this electrochemical method is its straightforward applicability to one-pot, orthogonal dual conjugation reactions by simply adjusting the applied voltages/charges.[36-38] To demonstrate this, we performed a one-pot, tandem electrochemical modification, leveraging orthogonal reactivity with Tyr. Since N-methyl luminol derivative (MeLum) has been reported as an effective reagent for electrochemical Tyr-selective bioconjugation,[25,28] we

used this reagent to target the Tyr residue of leuprorelin in our optimized setup. After Tyr modification with MeLum at 1.0 V, reagents for Trp-modification were added, and the reaction was further electrolyzed at 1.0 V. Each bioconjugation reagent selectively reacted with its target residues, producing doubly modified leuprorelin in 51% yield (Figure 4).

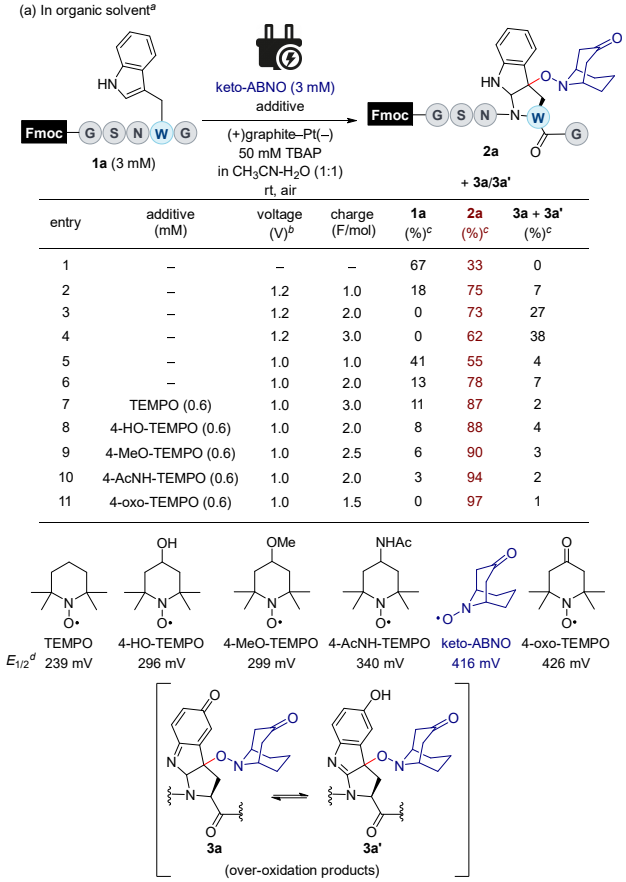

entry	additive (mM)	voltage (V)[b]	charge (F/mol)	1a (%)[c]	2a (%)[c]	3a + 3a' (%)[c]
1	–	–	–	67	33	0
2	–	1.2	1.0	18	75	7
3	–	1.2	2.0	0	73	27
4	–	1.2	3.0	0	62	38
5	–	1.0	1.0	41	55	4
6	–	1.0	2.0	13	78	7
7	TEMPO (0.6)	1.0	3.0	11	87	2
8	4-HO-TEMPO (0.6)	1.0	2.0	8	88	4
9	4-MeO-TEMPO (0.6)	1.0	2.5	6	90	3
10	4-AcNH-TEMPO (0.6)	1.0	2.0	3	94	2
11	4-oxo-TEMPO (0.6)	1.0	1.5	0	97	1

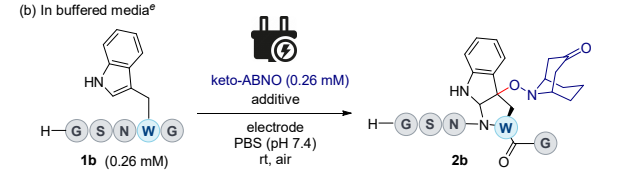

entry	additive (mM)	electrode	voltage (V)[f]	charge (F/mol)	1b (%)[c]	2b (%)[c]
1	4-oxo-TEMPO (0.52)	(+)graphite–Pt(–)	0.9	6.0	97	3
2	4-oxo-TEMPO (0.52)	(+)GC–GC(–)	0.9	4.0	59	37
3	4-oxo-TEMPO (0.26)	(+)GC–GC(–)	0.8	2.0	34	62
4	4-oxo-TEMPO (0.26) NaI (0.78)	(+)GC–GC(–)	0.8	2.0	2	88
5	4-oxo-TEMPO (0.26) NaBr (0.78)	(+)GC–GC(–)	0.8	2.0	0	94
6	4-oxo-TEMPO (0.26) NaCl (0.78)	(+)GC–GC(–)	0.8	2.0	18	76
7[g]	$NaNO_2$ (0.16)	-	-	-	0	70

Figure 1. Optimization of Electrochemical Trp-Selective Bioconjugation. [a] ElectraSyn 2.0 (IKA USA) potentiostat was utilized. [b] Ag/Ag^+ was used as the reference. [c] Yield was determined by HPLC analysis using UV detection at 230 nm. [d] The half-wave redox potentials ($E_{1/2}$ *vs* ferrocene) of *N*-oxyl radicals were cited from ref 35. [e] ECStat-301 (EC FRONTIER Co, Ltd.) potentiostat was utilized. [f] Ag/AgCl was used as the reference. [g] Chemical activation in 0.1% AcOH aq. (ref 31). Nitrosated **2b** was concomitantly produced in 17% yield.

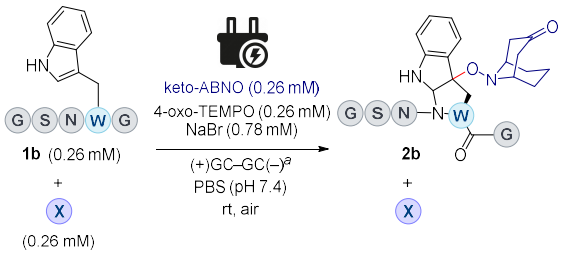

entry	X	voltage (V *vs* Ag/AgCl)	charge (F/mol)	yield (%)[b]	intact X (%)[b]
1	Bz-His-OH	0.6	4.0	77	97
2	Bz-Lys-OH	0.8	4.0	91	>99
3	Bz-Met-OH	0.8	4.0	88	>99
4	Bz-Tyr-OH	0.9	9.0	93	>99
5	$(Bz\text{-}Cys\text{-}OH)_2$ disulfide	0.8	4.0	96	>99

Figure 2. Amino Acid Compatibility. [a] ECStat-301 (EC FRONTIER Co, Ltd.) potentiostat was utilized. [b] Yield was determined by HPLC analysis using UV detection at 230 nm.

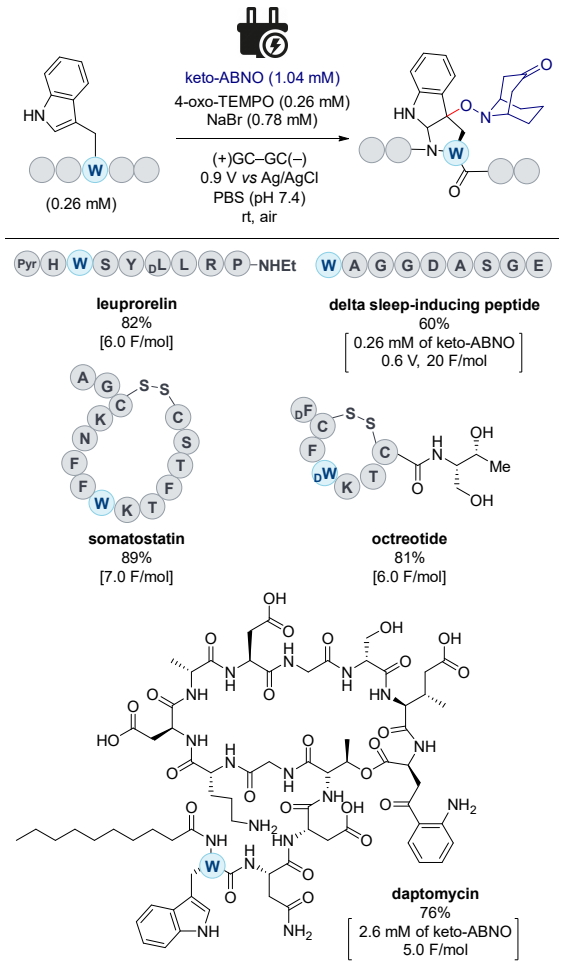

Figure 3. Electrochemical Trp-Modification of Peptides. ECStat-301 (EC FRONTIER Co, Ltd.) potentiostat was utilized. Yield was determined by HPLC analysis using UV detection at 230 nm.

The optimized buffered conditions were also applied to native proteins and a monoclonal antibody (trastuzumab) using a fluorescein isothiocyanate-conjugated reagent (FITC-ABNOH) (Figure 5). Labeling yield was determined by measuring fluorescence intensity on an SDS-PAGE gel. To achieve high conversion in the bioconjugation reaction, an excess of FITC-ABNOH (10-100 equivalents to proteins) was required, with 6.0-10 F/mol of electric charge applied at 0.85 V. SDS-PAGE analysis indicated minimal protein denaturation (Figure S23-S30).

Additionally, avidin pull-down experiments were conducted to confirm the preservation of payload function (Figure 6). In this experiment, a biotin-conjugated reagent (Biotin-ABNOH) was conjugated to Bovine Serum Albumin (BSA) under electrochemical conditions in PBS buffer. After conjugation, the binding capability of biotin to streptavidin beads was maintained, as demonstrated by a mock purification of the biotin-labeled BSA from a cell lysate mixture (Figure 6, lane D *vs.* lane E). These results indicate that the electrochemical Trp-bioconjugation method is broadly applicable to both protein and peptide substrates, and exhibits high tolerance to various functional groups. However, MS analysis frequently revealed overoxidation of protein conjugates, and applying higher electric charges often resulted in fluorescence bleaching of FITC. Reducing undesired overoxidation remains a challenge and is an area for further refinement in future applications.

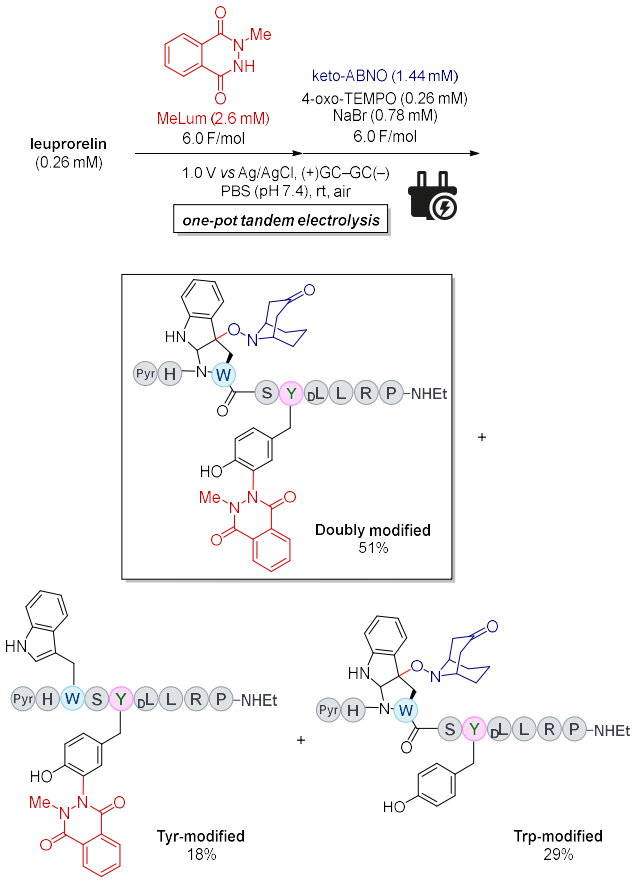

Figure 4. One-pot, Orthogonal, Dual Electrochemical Modifications. ECStat-301 (EC FRONTIER Co, Ltd.) potentiostat was utilized. Yield was determined by HPLC analysis using UV detection at 230 nm.

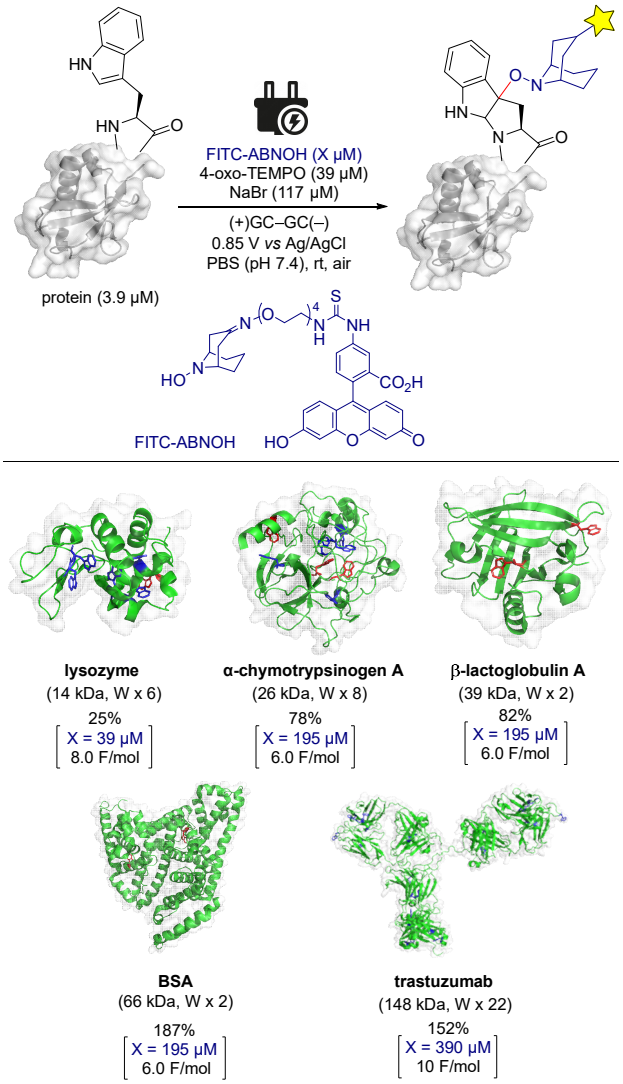

Figure 5. Electrochemical Trp-modification of proteins. ECStat-301 (EC FRONTIER Co, Ltd.) potentiostat was utilized. Assuming that the mono-conjugate product is obtained at 100% yield, yield was calculated from the fluorescence intensity of the SDS-PAGE bands using a calibration curve as a reference.

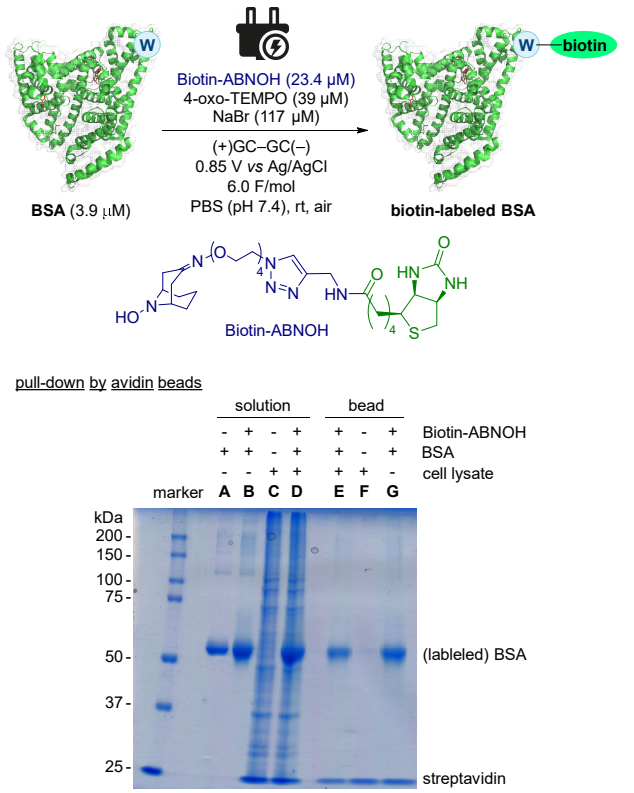

Figure 6. Biotin-labeled BSA was pulled down from a mixture with HeLa S3 cell lysate by utilizing streptavidin beads. The SDS-PAGE bands below 25kDa in lanes E-G correspond to streptavidin that was released from the beads upon boiling. Lane A: BSA alone, lane B: biotin-labeled BSA, lane C: HeLa S3 cell lysate, lane D: a mixture of cell lysate and biotin-labeled BSA used for the pull-down experiment, lane E: elution from streptavidin beads after pull down from the mixture of cell lysate and biotin-labeled BSA, wash with CRB (50 mM Tris-HCl (pH 7.5), 0.3% TritonX-100, 300 mM NaCl; 3 times), and boiling, lane F: elution from streptavidin beads treated with cell lysate without biotin-labeled BSA, wash with CRB (3 times), and boiling, lane G: elution from streptavidin beads treated with biotin-labeled BSA without cell lysate, wash with CRB (3 times), and boiling.

To gain insight into mechanism, we conducted systematic cyclic voltammetry (CV) measurements in PBS buffer (Figure 7). While Ac-Trp-OEt and keto-ABNO individually exhibited anodic peaks at 1.1 V and 0.8 V, respectively, a mixture of Ac-Trp-OEt and keto-ABNO displayed a new anodic peak at 0.68 V (Figure 7a).[39] This result indicates that Trp and keto-ABNO interact with each other, and the resulting complex (complex **B**) is more prone to oxidation than Ac-Trp-OEt or keto-ABNO alone. Another new anodic peak at 0.98 V is attributed to the Trp–keto-ABNO adduct. The cathodic peak currents disappeared due to the irreversible bioconjugation reaction occurring between the oxoammonium cation derived from keto-ABNO and Trp. However, in the case of Ac-Trp-OEt and 4-oxo-TEMPO, the cyclic voltammogram was a simple superposition of the two components (Figure S7a).[39] Thus, Trp and 4-oxo-TEMPO neither interact nor react. This is consistent with the absence of bioconjugation products observed between TEMPO or its derivatives and **1a**/**1b**. Using similar analysis, we could not observe electrochemical interactions between keto-ABNO and 4-oxo-TEMPO (Figure S7b).

Next, we examined the electrochemical interactions between NaBr and *N*-oxyl radicals. A solution containing NaBr and keto-ABNO produced a new anodic peak at 1.3 V, which is shifted to a lower potential compared to that of NaBr alone (1.4 V, Figure 7b). The same anodic peak at 1.3 V was also observed in the cyclic voltammogram of the mixture of NaBr and 4-oxo-TEMPO (Figure S7c). These anodic peaks at 1.3 V likely correspond to bromide anion ion-pairing with oxoammonium species ($R_2N{=}O^{+}\cdots Br^{-}$).[40]

In the cyclic voltammogram of a mixture of Ac-Trp-OEt, keto-ABNO, and NaBr (Figure 7c), two anodic peaks appeared at 0.68 V (Trp$\cdots$keto-ABNO) and 0.98 V (Trp–keto-ABNO adduct). The anodic peak at 1.3 V (keto-ABNO$^{+}\cdots Br^{-}$) and any cathodic peaks disappeared due to the consumption of keto-ABNO^{+} species via conjugation with Trp, which occurs quickly enough to complete within the sweeping timescale of CV. NaBr was not likely involved in the oxidation of keto-ABNO. These observations suggest a completely different mechanism from the previously proposed role of bromide in *N*-oxyl radical catalysis.[41] Bromide did not act as a redox mediator for the generation of oxoammonium species, because our bioconjugation proceeded under a constant voltage (0.8-0.9 V) below the oxidation potential of $R_2N{=}O^{+}\cdots Br^{-}$ (1.3 V) or NaBr (1.4 V). A mixture of Ac-Trp-OEt, 4-oxo-TEMPO, and NaBr produced the cyclic voltammogram that was a simple superposition of all three components, further supporting the electrochemical inertness of NaBr to the system (Figure 7d).

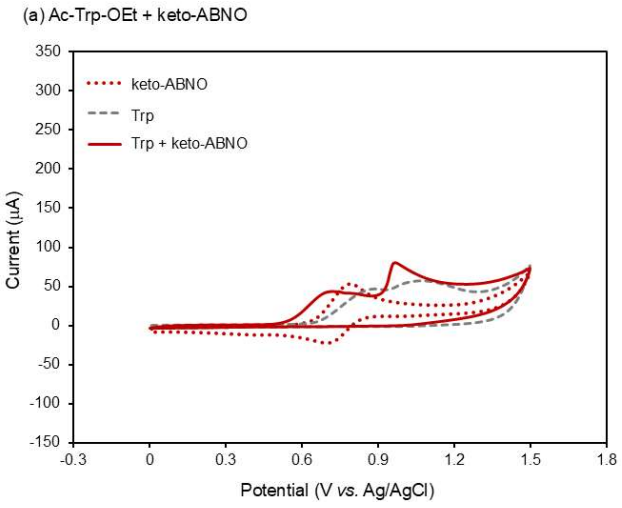

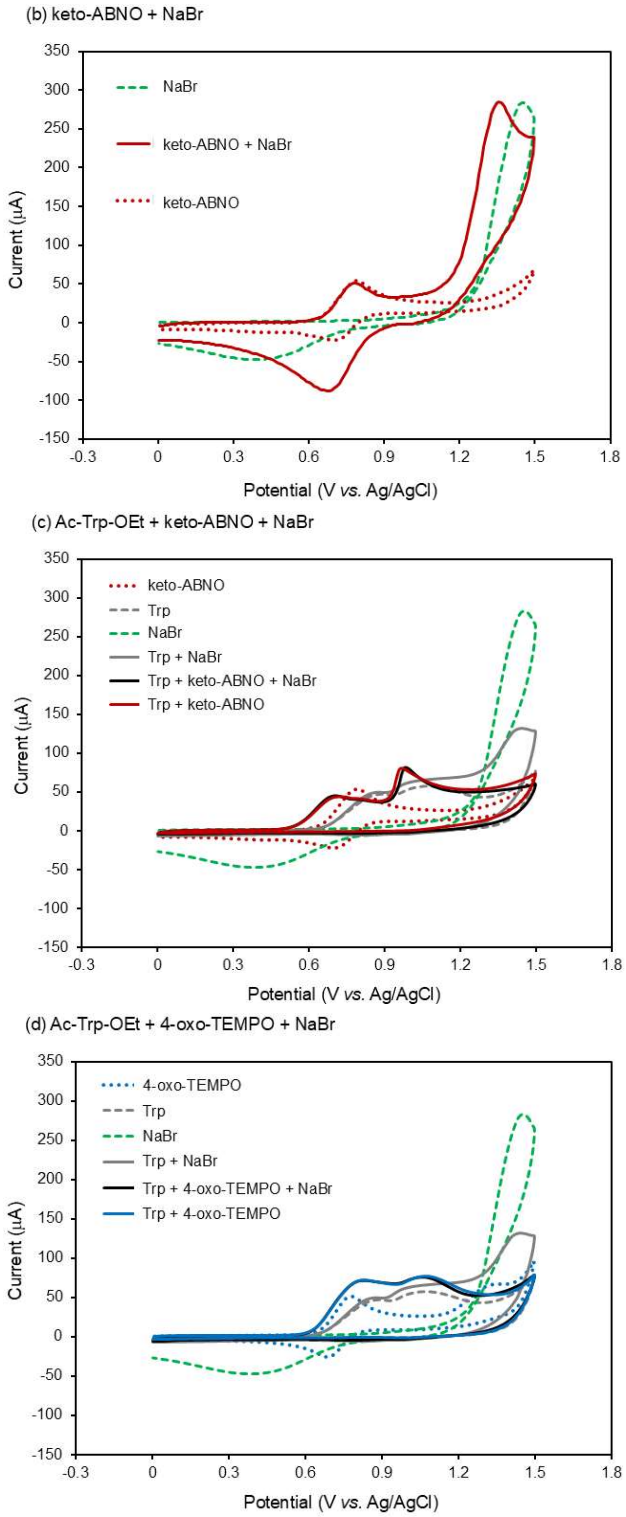

Figure 7. Cyclic voltammograms in PBS buffer (pH 7.4) on a glassy carbon working electrode at a scan rate of 100 mV s^{-1}. Concentration: Ac-Trp-OEt, keto-ABNO, 4-oxo-TEMPO = 3 mM; NaBr = 9 mM.

We further monitored the reaction profile of keto-ABNO and **1b** using LC-MS, varying the applied charge in the presence and absence of NaBr (Figure 8). At 0 F/mol, negligible reaction was observed in both cases after 5 minutes (<5% yield), indicating that electrical input is essential for driving the reaction, regardless of the presence of NaBr. As the applied charge increased, the reaction proceeded, with complete consumption of **1b** at 3.0 F/mol without NaBr and at 2.0 F/mol with NaBr. This outcome clearly demonstrates the accelerating effect of NaBr. Notably, in the absence of NaBr, significant formation of byproduct **3b** (the overoxidized **1b**–keto-ABNO adduct) was observed from the beginning of the reaction. The presence of NaBr significantly suppressed this side reaction, making the generation pathway of the active species preferred.

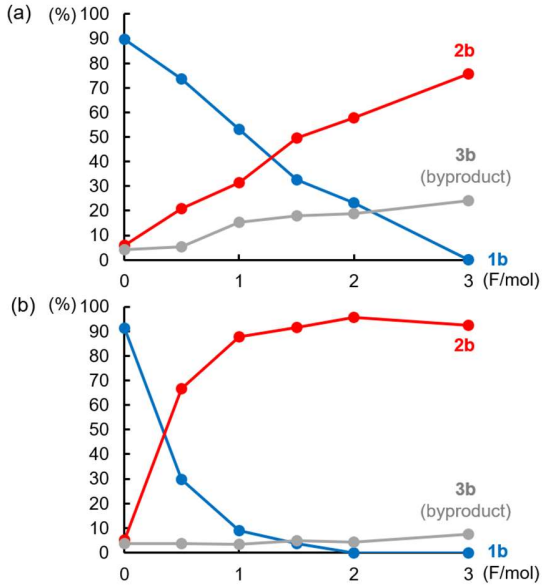

Figure 8. Reaction profiles for Trp-selective electrochemical bioconjugation of **1b**. (a) The profile in the absence of NaBr (Figure 1b, entry 4). (b) The profile in the presence of NaBr (0.78 mM; Figure 1b, entry 6). NaBr accelerated the bioconjugation and suppressed the side reaction producing over-oxidized byproduct **3b**.

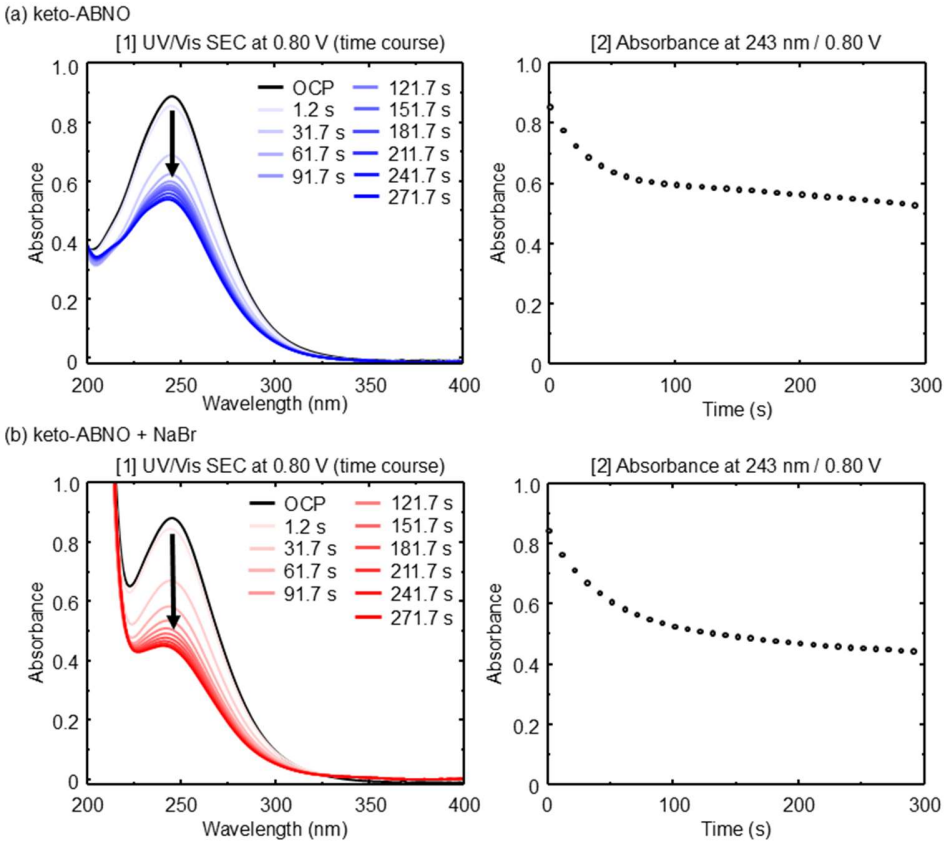

Figure 9. UV/Vis absorption spectral changes of (a) keto-ABNO and (b) keto-ABNO + NaBr, upon oxidation in degassed PBS buffer pH 7.4 (WE: Pt mesh; CE: Pt wire; RE: Ag/AgCl). All measurements were performed under an argon atmosphere. The concentration of keto-ABNO = 2.6 mM, NaBr = 7.9 mM. OCP = open circuit potential.

We further performed ultraviolet-visible (UV/Vis) absorption spectroelectrochemistry (SEC) measurements to investigate the electrochemical interactions between NaBr and *N*-oxyl radicals (Figure 9). UV/Vis absorption spectra were measured in degassed PBS buffer under an argon atmosphere. The spectra of keto-ABNO exhibited an absorption band (λ_{max} = 243 nm). Applying a potential of 0.80 V (*vs.* Ag/AgCl) to the keto-ABNO solution led to a decrease in the intensity of this absorption band, with an isosbestic point at 220 nm, suggesting the generation of a single active species throughout the electrolysis (Figure 9a-[1]). In the presence of NaBr, a similar trend was observed; the absorption band at 243 nm decreased upon applying a potential of 0.80 V, and the final profile of the band was comparable to that of keto-ABNO alone (Figure 9b-[1]). Additionally, the time courses of absorbance at 243 nm in the presence and absence of NaBr were nearly identical (Figures 9a-[2], 9b-[2]), indicating that the bromide anion does not accelerate the generation of active species through electrochemical interactions.

Multiple peaks were observed at approximately 220, 240, and 270 nm upon applying electric charge under air in the absence of NaBr, but the presence of NaBr significantly suppressed the generation of these peaks (Figure S9). These peaks likely originated from a decomposed form of keto-ABNO. In other words, the presence of bromide anions may direct charge usage away from the decomposition of active species and product overoxidation, thereby favoring the desired bioconjugation pathway.

Based the above experimental results, we propose a plausible reaction mechanism (Figure 10). Focusing on the generation of active species, keto-ABNO$^+$ (**A**), and the roles of the components, several factors should be considered. Firstly, an interaction between Trp and keto-ABNO is observed. Under a constant voltage of 0.8-0.9 V, electrochemical oxidation of Trp···keto-ABNO complex (**B**, E_{oxi} : 0.68 V)[42] reasonably generates the oxoammonium species **A**, promoting the bioconjugation process. Secondly, the presence of phosphate anions is found to inhibit the reaction, while the presence of a bromide anion restores reactivity. This is likely due to the favorable interaction between oxoammonium species and the bromide anion (depicted as **A**-Br and **C**), which helps prevent the decomposition of the active species without accelerating the generation of oxoammonium. This effect starkly contrasts with the previously proposed role of bromide anions in *N*-oxyl radical catalysis.[41] The two radicals, which have similar redox potentials but distinct steric demands, have distinct roles—keto-ABNO acts as a bioconjugation reagent, and 4-oxo-TEMPO functions as an electron mediator. 4-oxo-TEMPO may enhance the generation of the active oxoammonium species **A**-Br through oxidation of complex **B** existing in a low concentration in the solution phase and facilitate the productive bioconjugation process over the overoxidation pathway of product **2**. This alliance is critically important for achieving facile and high-yielding

electrochemical bioconjugation even in highly diluted conditions (sub-mM level). These synergistic roles of the components significantly suppress unproductive pathways that cause oxidative side reactions, possibly via direct oxidation on the electrodes.

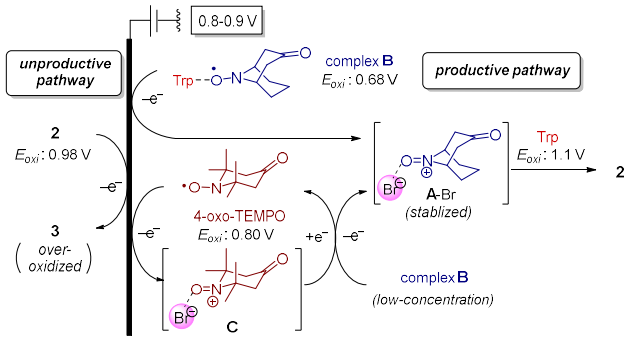

Figure 10. Plausible reaction mechanism. Oxidation potentials (E_{oxi}) are described *vs.* Ag/AgCl.

Conclusion

In conclusion, we successfully developed the first electrochemically promoted Trp-selective bioconjugation at protein scale by identifying a unique electrochemical cooperation among keto-ABNO, 4-oxo-TEMPO, and NaBr. This method offers advantages over the previous chemical activation approach using NO_x, as it can be performed in a neutral aqueous buffer. The accelerated reaction and reduced side reactions can be attributed to the unique role of NaBr, likely by stabilizing the oxoammonium active species. The reaction development described here may pave the way for novel processing techniques in the chemically modified biologics.[43]

ASSOCIATED CONTENT

Supporting Information. Experimental procedures, reaction setup, characterization data and analytical setup for CV and UV-SEC. The Supporting Information is available free of charge at https://pubs.acs.org.

AUTHOR INFORMATION

Corresponding Authors

Kounosuke Oisaki – Interdisciplinary Research Center for Catalytic Chemistry (IRC3), National Institute of Advanced Industrial Science and Technology (AIST), Tsukuba Central 5-2, 1-1-1 Higashi, Tsukuba, Ibaraki 305-8565, Japan; orcid.org/0000-0002-0499-8168; Email: k.oisaki@aist.go.jp

Motomu Kanai – Graduate School of Pharmaceutical Sciences, The University of Tokyo, 7-3-1 Hongo, Bunkyo-ku, Tokyo 113-0033, Japan; orcid.org/0000-0003-1977-7648; Email: motomukanai@g.ecc.u-tokyo.ac.jp

Authors

Ryo Kuroda– Graduate School of Pharmaceutical Sciences, The University of Tokyo, 7-3-1 Hongo, Bunkyo-ku, Tokyo 113-0033, Japan

Eisho Toyama – Graduate School of Pharmaceutical Sciences, The University of Tokyo, 7-3-1 Hongo, Bunkyo-ku, Tokyo 113-0033, Japan

Tomoya Sugai – International Institute for Integrative Sleep Medicine (WPI-IIIS), University of Tsukuba, 1-1-1 Tennodai, Tsukuba, Ibaraki 305-8575, Japan

Maho Imai – Department of Chemistry, School of Science, Institute of Science Tokyo, NE-6, 2-12-1 Ookayama, Meguro-ku, Tokyo 152-8550, Japan

Kohei Watanabe – Graduate School of Pharmaceutical Sciences, The University of Tokyo, 7-3-1 Hongo, Bunkyo-ku, Tokyo 113-0033, Japan

Natsuki Konoue – Graduate School of Pharmaceutical Sciences, The University of Tokyo, 7-3-1 Hongo, Bunkyo-ku, Tokyo 113-0033, Japan

Katsuya Maruyama – Graduate School of Pharmaceutical Sciences, The University of Tokyo, 7-3-1 Hongo, Bunkyo-ku, Tokyo 113-0033, Japan

Mio Kondo – Department of Chemistry, School of Science, Institute of Science Tokyo, NE-6, 2-12-1 Ookayama, Meguro-ku, Tokyo 152-8550, Japan

Shigeyuki Masaoka – Graduate School of Engineering, Osaka University, 2-1 Yamadaoka, Suita, Osaka, 565-0871 Japan

Tsuyoshi Saitoh – International Institute for Integrative Sleep Medicine (WPI-IIIS), University of Tsukuba, 1-1-1 Tennodai, Tsukuba, Ibaraki 305-8575, Japan

Author Contributions

The manuscript was written through contributions of all authors. / All authors have given approval to the final version of the manuscript. / ‡These authors contributed equally.

Funding Sources

This work was supported in part by JSPS KAKENHI [JP17H06442 (Hybrid Catalysis), JP17H01522, JP17K19479, JP20H00489, JP23H05466, JP23H04909 (Green Catalysis Science)] (for M.Ka.), JSPS KAKENHI [JP18H04239 (Precisely Designed Catalysts with Customized Scaffolding), JP18K06545, JP21H05077 (Glycan Chemical Knock-in), JP24K02160], JST [JPMJPF2017], Fugaku Trust for Medical Research, Astellas Foundation for Research on Metabolic Disorders, Research Grant from Noguchi Institute, Kobayashi Foundation for Cancer Research, Cancer Research Foundation, Takeda Science Foundation (for K.O.), JSPS KAKENHI [JP16H04125, JP17H06444 (Hybrid Catalysis), JP23H04903 (Green Catalysis Science) , JP24H00464] (for S.M.), JSPS KAKENHI [JP15H05480, JP17K19185, JP24H02212 (Chemical Structure Reprogramming (SReP))], JST FOREST [JPMJFR221S] (for M.Ko.), Iwadare Scholarship Foundation and JSPS Fellowship [JP21J14479] (for K.M.).

Notes

The authors declare no competing financial interest.

ABBREVIATIONS

ABNO, 9-azabicyclo[3.3.1]nonane-*N*-oxyl; TEMPO, 2,2,6,6-tetramethylpiperidine-*N*-oxyl; TBAP, *n*-tetrabutylammonium perchlorate; PBS, phosphate buffer saline; GC, glassy carbon; WE, working electrode; CE, counter electrode; RE, reference electrode; BSA, bovine serum albumin; CRB, cell resuspension buffer; CV, Cyclic voltammetry; SEC, spectroelectrochemistry.

REFERENCES

(1) Spicer, C. D.; Davis, B. G. Selective chemical protein modification. *Nat. Commun.* **2014**, *5*, 4740.

(2) deGruyter, J. N.; Malins, L. R.; Baran, P. S. Residue-Specific Peptide Modification: A Chemist's Guide. *Biochemistry* **2017**, *56(30)*, 3863–3873.

(3) Maruyama, K.; Kanai, M. Synthetic Methodology-Driven Chemical Protein Modifications. *Chem. Lett.* **2019**, *48(11)*, 1421–1432.
(4) Hoyt, E. A.; Cal, P. M. S. D.; Oliveira, B. L.; Bernardes, G. J. L. Contemporary Approaches to Site-Selective Protein Modification. *Nat. Rev. Chem.* **2019**, *3(3)*, 147–171.
(5) Shadish, J. A.; DeForest, C. A. Site-Selective Protein Modification: From Functionalized Proteins to Functional Biomaterials. *Matter* **2020**, *2(1)*, 50–77.
(6) Kjærsgaard, N. L.; Nielsen, T. B.; Gothelf. K. V. Chemical Conjugation to Less Targeted Proteinogenic Amino Acids. *ChemBioChem* **2022**, *23(19)*, e202200245.
(7) Chauhan, P.; V. Ragendu; Kumar, M.; Molla, R.; Mishra, S. D.; Basa, S.; Rai, V. Chemical technology principles for selective bioconjugation of proteins and antibodies. *Chem. Soc. Rev.* **2024**, *53*, 380-449.
(8) Alvarez Dorta, D.; Deniaud, D.; Mével, M.; Gouin, S. G. Tyrosine Conjugation Methods for Protein Labelling. *Chem. Eur. J.* **2020**, *26(63)*, 14257–14269.
(9) Szijj, P. A.; Kostadinova, K. A.; Spears, R. J.; Chudasama, V. Tyrosine Bioconjugation - an Emergent Alternative. *Org. Biomol. Chem.* **2020**, *18(44)*, 9018–9028.
(10) Chatterjee, J.; Bandyopadhyay, A.; Pattabiraman, M.; Sarkar R. *Chem. Commun.* **2024**, *60*, 8978-8996.
(11) Hu, J.-J.; He, P.-Y.; Li, Y.-M. Chemical Modifications of Tryptophan Residues in Peptides and Proteins. *J. Pept. Sci.* **2021**, *27(1)*, e3286.
(12) Zang, J.; Chen, Y.; Zhu, W.; Lin, S. Chemoselective Methionine Bioconjugation on a Polypeptide, Protein, and Proteome. *Biochemistry* **2020**, *59(2)*, 132–138.
(13) Yan, M.; Kawamata, Y.; Baran, P. S. Synthetic Organic Electrochemical Methods Since 2000: On the Verge of a Renaissance. *Chem. Rev.* **2017**, *117(21)*, 13230–13319.
(14) Wiebe, A.; Gieshoff, T.; Möhle, S.; Rodrigo, E.; Zirbes, M.; Waldvogel, S. R. Electrifying Organic Synthesis. *Angew. Chem. Int. Ed.* **2018**, *57(20)*, 5594–5619.
(15) Möhle, S.; Zirbes, M.; Rodrigo, E.; Gieshoff, T.; Wiebe, A.; Waldvogel, S. R. Modern Electrochemical Aspects for the Synthesis of Value-Added Organic Products. *Angew. Chem. Int. Ed.* **2018**, *57(21)*, 6018–6041.
(16) Shatskiy, A.; Lundberg, H.; Kärkäs, M. D. Organic Electrosynthesis: Applications in Complex Molecule Synthesis. *ChemElectroChem* **2019**, *6(16)*, 4067–4092.
(17) Zhu, C.; Ang, N. W. J.; Meyer, T. H.; Qiu, Y.; Ackermann, L. Organic Electrochemistry: Molecular Syntheses with Potential. *ACS Cent. Sci*. **2021**, *7(3)*, 415–431.
(18) Weng, Y.; Song, C.; Chiang, C.-W.; Lei, A. Single Electron Transfer-Based Peptide/Protein Bioconjugations Driven by Biocompatible Energy Input. *Commun. Chem.* **2020**, *3(1)*, 1–11.
(19) Mackay, A. S.; Payne, R. J.; Malins, L. R. Electrochemistry for the Chemoselective Modification of Peptides and Proteins. *J. Am. Chem. Soc.* **2022**, *144(1)*, 23–41.
(20) Walton, D. J.; Heptinstall, J. Electrochemical Modification of Proteins. A Review. *Prep. Biochem. Biotechnol.* **2000**, *30(1)*, 1–14.
(21) Kendall, G.; Cooper, H. J.; Heptinstall, J.; Derrick, P. J.; Walton, D. J.; Peterson, I. R. Specific Electrochemical Nitration of Horse Heart Myoglobin. *Arch. Biochem. Biophys.* **2001**, *392(2)*, 169–179.
(22) Takahashi, M.; Handa, A.; Yamaguchi, Y.; Kodama, R.; Chiba, K. Anodic Oxidative Modification of Egg White for Heat Treatment. *J. Agric. Food Chem.* **2016**, *64(34)*, 6503–6507.
(23) van den Brink, F. T. G.; Zhang, T.; Ma, L.; Bomer, J.; Odijk, M.; Olthuis, W.; Permentier, H. P.; Bischoff, R.; van den Berg, A. Electrochemical Protein Cleavage in a Microfluidic Cell with Integrated Boron Doped Diamond Electrodes. *Anal. Chem.* **2016**, *88(18)*, 9190–9198.
(24) Alvarez-Dorta, D.; Thobie-Gautier, C.; Croyal, M.; Bouzelha, M.; Mével, M.; Deniaud, D.; Boujtita, M.; Gouin, S. G. Electrochemically Promoted Tyrosine-Click-Chemistry for Protein Labeling. *J. Am. Chem. Soc.* **2018**, *140(49)*, 17120–17126.
(25) Depienne, S.; Alvarez-Dorta, D.; Cryoyal, M.; Temgoua, R. C. T.; Charlier, C.; Deniaud, D.; Mével, M.; Boujtita, M.; Gouin, S. G. *Chem. Sci.* **2021**, *12*, 15374-15381.
(26) Depienne, S.; Bouzelha, M.; Courtois, E.; Pavageau, K.; Lalys, P.-A.; Marchand, M.; Alvarez-Dorta, D.; Nedellec, S.; Marín-Fernández, L.; Grandjean, C.; Boujtita, M.; Deniaud, D.; Mével, M.; Gouin, S. G. *Nat. Commun.* **2023**, *14*, 5122.
(27) Song, C.; Liu, K.; Wang, Z.; Ding, B.; Wang, S.; Weng, Y.; Chiang, C.-W.; Lei, A. Electrochemical Oxidation Induced Selective Tyrosine Bioconjugation for the Modification of Biomolecules. *Chem. Sci.* **2019**, *10(34)*, 7982–7987.
(28) Sato, S.; Matsumura, M.; Kadonosono, T.; Abe, S.; Ueno, T.; Ueda, H.; Nakamura, H. Site-Selective Protein Chemical Modification of Exposed Tyrosine Residues Using Tyrosine Click Reaction. *Bioconjug. Chem.* **2020**, *31(5)*, 1417–1424.
(29) Weng, Y.; Xu, X.; Chen, H.; Zhang, Y.; Zhuo, X. Tandem Electrochemical Oxidative Azidation/Heterocyclization of Tryptophan-Containing Peptides under Buffer Conditions. *Angew. Chem. Int. Ed*. **2022**, *61(41)*, e202206308.
(30) Kawamata, Y.; Ryu, K. A.; Hermann, G. N.; Sandahl, A.; Vantourout, J. C.; Olow, A. K.; Adams, L.-T. A.; Rivera-Chao, E.; Roberts, L. R.; Gnaim, S.; Nassir, M.; Oslund, R. C.; Fadeyi, O. O.; Baran, P. S. An electroaffinity labelling platform for chemoproteomic-based target identification. *Nat. Chem.* **2023**, *15*, 1267-1275.
(31) Seki, Y.; Ishiyama, T.; Sasaki, D.; Abe, J.; Sohma, Y.; Oisaki, K.; Kanai, M. Transition Metal-Free Tryptophan-Selective Bioconjugation of Proteins. *J. Am. Chem. Soc.* **2016**, *138 (34)*, 10798–10801.
(32) Maruyama, K.; Malawska, K. J.; Konoue, N.; Oisaki, K.; Kanai, M. Synthesis of Tryptophan–Folate Conjugates. *Synlett* **2020**, *31 (08)*, 784–787.
(33) Nutting, J. E.; Rafiee, M.; Stahl, S. S. Tetramethylpiperidine N-Oxyl (TEMPO), Phthalimide *N*-Oxyl (PINO), and Related *N*-Oxyl Species: Electrochemical Properties and Their Use in Electrocatalytic Reactions. *Chem. Rev.* **2018**, *118 (9)*, 4834–4885.
(34) This background reaction may proceed via the disproportionation of keto-ABNO to oxoammonium cation **A**, facilitated by the C-terminal carboxylic acid of **1a**. Under identical conditions, Ac-Trp-OEt did not induce any background reaction. For further information on the acidic disproportionation of *N*-oxyl radicals, see: (a) Kishioka, S.-y.; Ohsaka, T.; Tokuda, K. Electrochemical studies of acid-promoted disproportionation of nitroxyl radical. *Electrochim. Acta* **2003**, *48(11)*, 1589-1594. (b) Sen', V. D.; Golubev, V. A. Kinetics and mechanism for acid-catalyzed disproportionation of 2,2,6,6-tetramethylpiperidine-1-oxyl. *J. Phys. Org. Chem.* **2009**, *22(2)*, 138-143. (c) Sen', V. D.; Tikhonov, I. V.; Borodin, L. I.; Pliss, E. M.; Golubev, V. A.; Syroeshkin, M. A.; Rusakov, A. I. Kinetics and thermodynamics of reversible disproportionation–comproportionation in redox triad oxoammonium cations – nitroxyl radicals – hydroxylamines. *J. Phys. Org. Chem.* **2015**, *28(1)*, 17-24.
(35) Lauber, M. B.; Stahl, S. S. Efficient Aerobic Oxidation of Secondary Alcohols at Ambient Temperature with an ABNO/NO_x Catalyst System. *ACS Catal.* **2013**, *3(11)*, 2612–2616.
(36) Maruani, A.; Richards, D. A.; Chudasama, V. Dual Modification of Biomolecules. *Org. Biomol. Chem.* **2016**, *14 (26)*, 6165–6178.
(37) Xu, L.; Kuan, S. L.; Weil, T. Contemporary Approaches for Site-Selective Dual Functionalization of Proteins. *Angew. Chem. Int. Ed.* **2021**, *60 (25)*, 13757-13777.
(38) For consecutive electrochemical reactions in one pot in small molecule synthesis, see: (a) Suga, S.; Watanabe, M.; Yoshida, J.-i. Electroauxiliary-Assisted Sequential Introduction of Two Carbon Nucleophiles on the Same α-Carbon of Nitrogen: Application to the Synthesis of Spiro Compounds. *J. Am. Chem. Soc.* **2002**, *124(50)*, 14824–14825. (b) Suga, S.; Watanabe, M.; Song, C.-H.; Yoshida, J.-i. Electroauxiliary-Assisted Sequential Introduction of Organic Groups on the α-Carbons of Nitrogen. *Electrochemistry* **2006**, *74(8)*, 672–679. (c) Nokami, T.; Hayashi, R.; Saigusa, Y.; Shimizu, A.; Liu, C.-Y.; Mong, K.-K. T.; Yoshida, J.-i. Automated Solution-Phase Synthesis of Oligosaccharides via Iterative Electrochemical Assembly of Thioglycosides. *Org. Lett.* **2013**, *15(17)*, 4520–4523. (d) Nokami,

T.; Isoda, Y.; Sasaki, N.; Takaiso, A.; Hayase, S.; Itoh, T.; Hayashi, R.; Shimizu, A.; Yoshida, J.-i. Automated Electrochemical Assembly of the Protected Potential TMG-chitotriomycin Precursor Based on Rational Optimization of the Carbohydrate Building Block. *Org. Lett.* **2015**, *17(6)*, 1525−1528. (e) Nokami, T.; Tsuyama, H.; Shibuya, A.; Nakatsutsumi, T. Oligosaccharide Synthesis Based on a One-pot Electrochemical Glycosylation–Fmoc Deprotection Sequence. *Chem. Lett.* **2008**, *37(9)*, 942−943. (f) Hartmer, M. F.; Waldvogel, S. R. Electroorganic synthesis of nitriles via a halogen-free domino oxidation–reduction sequence. *Chem. Commun.* **2015**, *51*, 16346−16348. (g) Kawabata, Y.; Naito, Y.; Saitoh, T.; Kawa, K.; Fuchigami, T.; Nishiyama, S. Synthesis of (+)-O-Methylthalibrine by Employing a Stereocontrolled Bischler–Napieralski Reaction and an Electrochemically Generated Diaryl Ether. *Eur. J. Org. Chem.* **2014**, *1*, 99-104.

(39) The reason for the absence of cathodic peaks of Ac-Trp-OEt is due to the electrode coating by directly oxidized Trp. See discussions in section 7-3 of Supporting Information.

(40) We hypothesized that lowering the oxidation potential of Br^- by interacting with the oxoammonium cation would be analogous to previous reports that $TEMPO^+\cdots N_3^-$ interactions also lowered the oxidation potential of N_3^-. Siu, J. C.; Sauer, G. S.; Saha, A.; Macey, E. L.; Fu, N.; Chauviré, T.; Lancaster, K. M.; Lin, S. Electrochemical Azidooxygenation of Alkenes Mediated by a TEMPO–N_3 Charge-Transfer Complex. *J. Am. Chem. Soc.* **2018**, *140(39)*, 12511−12520.

(41) Several papers described that *N*-oxyl radical-catalyzed chemical/electrochemical oxidation was significantly accelerated in the presence of bromide anion, which was often proposed as a redox mediator for generating oxoammonium species without systematic CV analysis: (a) Anelli, P. L.; Biffi, C.; Montanari, F.; Quici, S. Fast and Selective Oxidation of Primary Alcohols to Aldehydes or to Carboxylic Acids and of Secondary Alcohols to Ketones Mediated by Oxoammonium Salts under Two-Phase Conditions. *J. Org. Chem.* **1987**, *52(12)*, 2559−2562. (b) Inokuchi, T.; Matsumoto, S.; Torii, S. Indirect electrooxidation of alcohols by a double mediatory system with two redox couples of $[R_2N^+{=}O]/R_2NO^\cdot$ and $[Br^\cdot$ or $Br^+]/Br^-$ in an organic-aqueous two-phase solution. *J. Org. Chem.* **1991**, *56(7)*, 2416-2421. (c) Demizu, Y.; Shiigi, H.; Oda, T.; Matsumura, Y.; Onomura, O. Efficient oxidation of alcohols electrochemically mediated by azabicyclo-N-oxyls. *Tetrahedron Lett.* **2008**, *49(1)*, 48-52.

(42) Structural studies of how keto-ABNO interacts with Trp in aqueous solvent are difficult due to the transient and radical characteristics. The following two types of interactions may be operative based on previous reports; (i) For hydrogen-bonding interactions of *N*-oxyl radical and indole in organic solvent, see: (a) Qui, Z. W.; Grant, D. M.; Pugmire, R. J. Paramagnetic carbon-13 shifts induced by the free radical Tempo. 2. Nitrogen heterocycles. *J. Am. Chem. Soc.* **1984**, *106(3)*, 557-563. (ii) For radical-π interaction, see: (b) Estarellas, C.; Frontera, A.; Quiñonero, D.; Deyà, P. M. Radical cation ($C^{\cdot+}$–π) and radical anion ($A^{\cdot-}$–π) interactions with aromatic rings: energetic, orbitalic and spin density considerations. *Phys. Chem. Chem. Phys.* **2011**, *13*, 16698-16705.

(43) Houser D.; Beaver S. Automating ADC Manufacturing with Electricity. *J. ADC.* April 10, 2023. DOI: 10.14229/jadc.2023.04.10.001.

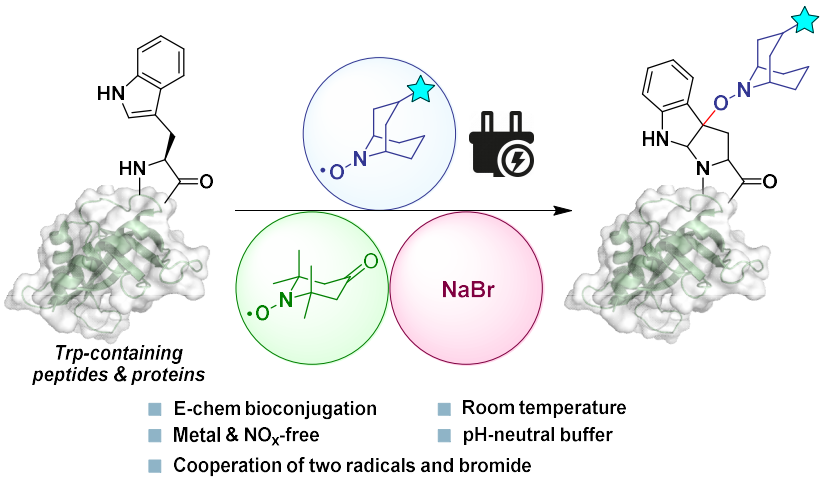

- E-chem bioconjugation
- Metal & NO_x-free
- Cooperation of two radicals and bromide
- Room temperature
- pH-neutral buffer